

LATENT DEGRADATION REPRESENTATION CONSTRAINT FOR SINGLE IMAGE DERAINING

Yuhong He*, Long Peng*, Lu Wang†, Jun Cheng

ABSTRACT

Since rain streaks show a variety of shapes and directions, learning the degradation representation is extremely challenging for single image deraining. Existing methods are mainly targeted at designing complicated modules to implicitly learn latent degradation representation from coupled rainy images. This way, it is hard to decouple the content-independent degradation representation due to the lack of explicit constraint, resulting in over- or under-enhancement problems. To tackle this issue, we propose a novel Latent Degradation Representation Constraint Network (LDRCNet) that consists of Direction-Aware Encoder (DAEncoder), UNet Deraining Network, and Multi-Scale Interaction Block (MSIBlock). Specifically, the DAEncoder is proposed to adaptively extract latent degradation representation by using the deformable convolutions to exploit the direction consistency of rain streaks. Next, a constraint loss is introduced to explicitly constraint the degradation representation learning during training. Last, we propose an MSIBlock to fuse with the learned degradation representation and decoder features of the deraining network for adaptive information interaction, which enables the deraining network to remove various complicated rainy patterns and reconstruct image details. Experimental results on synthetic and real datasets demonstrate that our method achieves new state-of-the-art performance. The source code will be publicly available.

Index Terms— Single Image Deraining, Representation Constraint, Deformable Convolution, Interactive Feature Fusion

1. INTRODUCTION

Images captured in rainy scenes will introduce artifacts like rain streaks, which would lead to a loss of image detail and contrast. This will degrade the performance of outdoor computer vision systems, such as autonomous driving [1] and video surveillance [2]. Therefore, restoring rainy images is an essential pre-processing step for outdoor computer vision applications, and it has drawn much attention in recent years [3, 4, 5, 6]. However, single image deraining is still very challenging due to the difficulty of learning the degradation representation of rain streaks in different scenarios [7].

Traditional methods usually solve this problem by calculating a mathematical statistic to obtain diverse priors by exploring the physical properties of rain streaks [8, 9]. However, traditional methods have difficulty in dealing with complex rainy images in real scenarios. Therefore, many deep learning-based methods have recently been proposed for single image deraining and achieved better performance [10, 11, 12, 13, 14, 15]. For example, according to the direction property of rain streaks, Wang *et al.* [10] proposed a spatial attentive network to remove rain streaks in a local-to-global manner. Ma *et al.* [14] proposed to integrate degradation learning by an iterative framework. Albeit these methods made significant progress, they still suffer from performance bottlenecks. This is because rain streaks and background are tightly coupled while existing methods

focus on designing various modules to learn the degradation representation implicitly and are unable to decouple content-independent degradation representation, which would result in insufficient rain streaks residual (*i.e.* under-enhancement) or smooth image textures (*i.e.* over-enhancement). Thus, explicit latent degradation representation learning is critical for single image deraining, which can handle spatially varying rainy patterns in different scenarios and adaptively enhance the structural information to decouple rainy images [16].

To achieve this goal, we propose a novel Latent Degradation Representation Constraint Network (LDRCNet) to remove rain streaks and enhance image details adaptively. Specifically, we propose a direction-aware encoder (DAEncoder) to extract the latent degradation representation by utilizing deformable convolution [17], which is inspired by the directional consistency of rain streaks in local region [18] and the directional perception capacity of deformable convolution [19, 20]. To explicitly supervise the latent degradation representation, we introduce a constraint framework by taking the original clean image and the latent degradation representation learned by the DAEncoder to reconstruct the corresponding rainy image during training. In this way, the latent degradation representation is encouraged to disentangle the content-independent representation of rain degradation by optimizing the loss between the reconstructed result and the rainy image. To provide additional information to the deraining network for decoupling the rain degradation layer and clean background, we propose a Multi-Scale Interaction Block (MSIBlock) to fuse the content-independent degradation representation and content-dependent decoder features of the deraining network. Such adaptive information interaction enables the deraining network to effectively handle various and complicated rainy patterns and reconstruct the details of images, and our deraining network adopts a simple yet effective U-Net architecture without fancy design. The training process of our LDRCNet is divided into two steps. We first learn the multi-scale latent degradation representation through the DAEncoder and the constraint framework, and then we freeze the DAEncoder to extract latent degradation representation to train the deraining network.

The contributions can be summarized as follows: (1) We propose a novel Latent Degradation Representation Constraint Network (LDRCNet), which utilizes the Direction-Aware Encoder (DAEncoder) to learn the direction-aware degradation representation of rain streaks and provides the explicit constraint by constraint framework. (2) We propose a novel Multi-Scale Feature Interaction Block (MSIBlock) that fuses learned degradation representation and decoder features of deraining networks to handle complex rain scenarios and reconstruct image details adaptively. (3) Experiments on synthetic and real-world datasets demonstrate that LDRCNet achieves new state-of-the-art performance with the latent degradation representation constraint and adaptive information interaction.

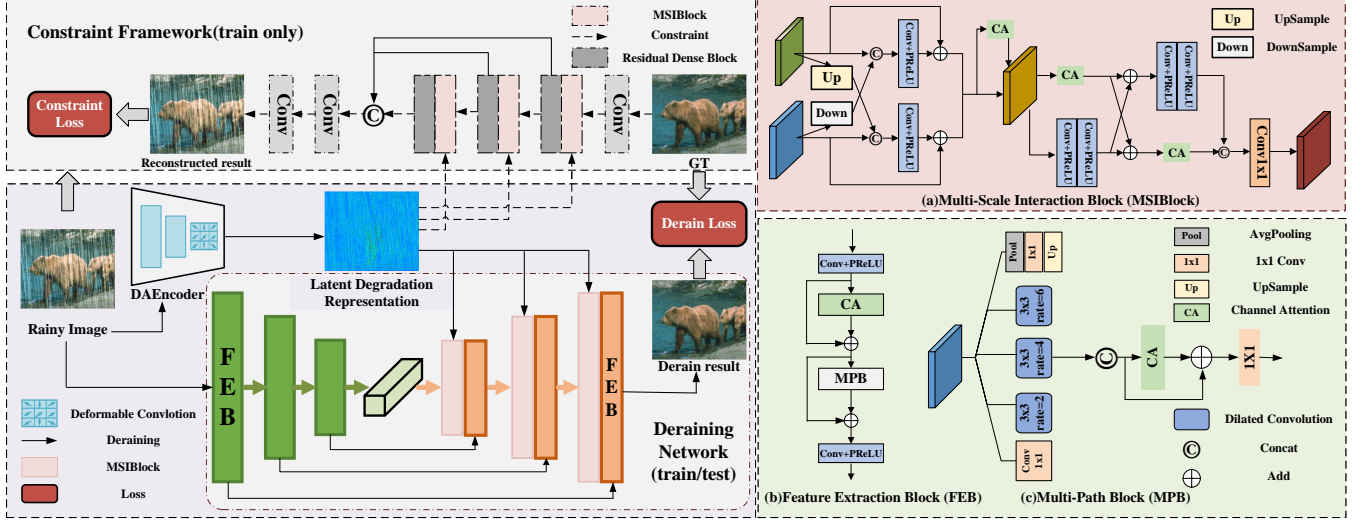


Fig. 1. Our proposed LDRCNet consists of the Direction-Aware Encoder (DAEncoder), Deraining Network, and Multi-Scale Interaction Block (MSIBlock). The constraint framework is proposed to provide explicit supervision to DAEncoder.

2. RELATED WORK

Existing single image deraining methods can be divided into two categories: traditional and deep learning-based methods [21, 22]. Traditional methods mainly introduce various priors to provide additional constraint, such as Gaussian mixture model-based prior [8], sparsity-based prior [9] and high-frequency prior [23]. However, these methods can only deal with specific rainy situations, resulting in poor generalization ability. Recently, numerous deep-learning methods have been proposed and achieved excellent performance [24, 25, 26, 27, 28, 29]. For example, Zhang *et al.* [30] proposed a density-aware multi-stream dense network to better characterize rain streaks with different scales and shapes. Jiang *et al.* [31] proposed to explore the multi-scale collaborative representation of rain streaks. In [32], a multi-stage architecture is proposed to learn the restoration function of degraded inputs. Ye *et al.* [4] proposed to jointly learn rain generation and removal procedure within a unified disentangled image translation framework. Leveraging the Transformer’s capability of capturing the long-range dependency [33], Xiao *et al.* [34] designed an effective transformer-based architecture that can capture long-range and complicated rainy information. Albeit these methods achieve great performance by designing various modules to learn the degradation representation of rain streaks from rainy images that couple rain degradation and the clean background, they still have difficulty in learning content-independent degradation representation without explicit constraint to enhance the structural details, resulting in over- and under-enhancement problems.

3. PROPOSED METHOD

In this work, we propose a novel Latent Degradation Representation constraint Network (LDRCNet), as shown in Fig. 1. We design a Direction-Aware Encoder (DAEncoder) to perceive the directional properties of rain streaks and extract the latent degradation representation, and a constraint framework is proposed to provide explicit supervision. To effectively take advantage of the learned degradation representation for separating the rain layer and background, a Multi-Scale Feature Interaction Block (MSIBlock) is proposed for both the constraint framework and the deraining network.

3.1. Latent Degradation Representation Learning

Direction-Aware Encoder. Inspired by the observation of the direction consistency of rain streaks in local regions, we propose the DAEncoder consists of several deformable convolutions[17] to learn multi-scale direction-aware degradation representation $deg = \{deg_1, deg_2, deg_3\}$ from the rainy image R , and they represent degradation representation at different scales. Specifically, deformable convolution can adjust the receptive field of the convolution kernel to adapt to the actual geometric variations of the rain streaks by using learnable offsets, which are used to extract the latent degradation representation of rain streaks with different shapes and directions adaptively. For each location p_0 on the output feature map y , deformable convolution can be formulated as:

$$y(p_0) = \sum_{p_l \in L} w(p_l) \cdot x(p_0 + p_l + \Delta p_l) \quad (1)$$

where p_l enumerates the offset relative to the kernel center p_0 , which is in $L = \{(-1, -1), \dots, (1, 1)\}$. For example, L has nine choices for a 3×3 convolution kernel. w represents the weight of different locations. Compared with ordinary convolution, deformable convolution has an augmented offset Δp_l , which can be learned from the data to adapt to the different directions of rain streaks. Finally, the learning process of DAEncoder can be expressed as:

$$\{deg_1, deg_2, deg_3\} = E(R) \quad (2)$$

Constraint Framework. Most existing deraining methods learn the latent degradation representation of rain streaks implicitly, which may result in insufficient rain streaks residual or image textures being smoothed. To tackle this issue, we propose a constraint framework to explicitly constrain the learning process of degradation representation. Specifically, the framework learns to reconstruct the corresponding rainy image \hat{R} from the input of the original clean image B and the multi-scale degradation representation. We introduce a constraint loss \mathcal{L}_C to optimize the loss between the reconstructed result and the original rainy image. In this way, the latent degradation representation learned by the DAEncoder can be supervised by the original rainy image R , which makes it tend to the content-independent representation of rain degradation. The

Table 1. Quantitative comparisons with existing state-of-the-art deraining methods. Average means the average performance of the five benchmark datasets. The **bold** and underline represent the best and second-best performance.

Metrics	Test100		Rain100H		Rain100L		Test1200		Test2800		Average	
	PSNR	SSIM	PSNR	SSIM	PSNR	SSIM	PSNR	SSIM	PSNR	SSIM	PSNR	SSIM
DerainNet[35]	22.77	0.810	14.92	0.592	27.03	0.884	23.38	0.835	24.31	0.861	22.48	0.796
SEMI[24]	22.35	0.788	16.56	0.486	25.03	0.842	26.05	0.822	24.43	0.782	22.88	0.744
DIDMDN[30]	22.56	0.818	17.35	0.524	25.23	0.741	29.95	0.901	28.13	0.867	24.64	0.770
URML[25]	24.41	0.829	26.01	0.832	29.18	0.923	30.55	0.910	29.97	0.905	28.02	0.880
RESCAN[26]	25.00	0.835	26.36	0.786	29.80	0.881	30.51	0.882	31.29	0.904	28.59	0.858
SPANet[10]	23.17	0.833	26.54	0.843	32.20	0.951	31.36	0.912	30.05	0.922	28.66	0.892
PReNet[27]	24.81	0.851	26.77	0.858	32.44	0.950	31.36	0.911	31.75	0.916	29.43	0.897
MSPFN[31]	27.50	0.876	28.66	0.860	32.40	0.933	32.39	0.916	32.82	0.930	30.75	0.903
CRDNet[11]	27.72	0.887	28.63	0.872	33.28	0.952	32.44	0.913	33.39	0.935	31.09	0.912
MPRNet[32]	<u>30.27</u>	0.897	<u>30.41</u>	0.890	36.40	0.965	32.91	<u>0.916</u>	<u>33.64</u>	<u>0.938</u>	<u>32.73</u>	0.921
IDLIR[14]	28.33	0.894	29.33	0.886	35.72	0.965	32.06	0.917	32.93	0.936	31.67	0.920
Uformer-B[13]	29.90	<u>0.906</u>	30.31	0.900	36.86	0.972	29.45	0.903	33.53	0.939	32.01	0.924
IDT[34]	29.69	0.905	29.95	<u>0.898</u>	37.01	<u>0.971</u>	31.38	0.908	33.38	0.937	32.28	<u>0.924</u>
Semi-SwinDerain[36]	28.54	0.893	28.79	0.861	34.71	0.957	30.96	0.909	32.68	0.932	31.14	0.910
LDRNet(Ours)	31.19	0.913	30.60	0.892	36.73	0.967	<u>32.89</u>	0.917	33.67	0.939	33.02	0.926

constraint framework structure is based on several Residual Dense Blocks (RDB) [37] and MSIBlock, as shown in Fig. 1. The RDB can maximize the information flow and better realize feature reuse and the MSIBlock is described in detail in Section 3.2.

The constraint framework C is only used in the training phase and the learning process and the loss function can be expressed as:

$$\mathcal{L}_C(R, \hat{R}) = \mathcal{L}(R, C(B, deg)) \quad (3)$$

3.2. Deraining with Learned Degradation Representation

To let the deraining network adaptively decouple rain streaks in complicated scenes and recover the details of the images, we use MSIBlock to interact the learned content-independent degradation representation of rain streaks with the content-dependent decoder features of the deraining network for adaptive feature fusion.

Deraining Network. Rich multi-scale representation has fully demonstrated its effectiveness in removing rain streaks [31]. Therefore, we use a simple yet effective U-Net architecture as the deraining network to extract feature maps at different scales. To retrieve more contextual information, we further propose a Multi-Path Block (MPB) in each feature extraction layer to aggregate more features of rain streaks with a larger receptive field. The MPB has several branches to enlarge the receptive field in parallel, as shown in Fig. 1 (c). In particular, the MPB first utilizes 1×1 convolution, avgpooling, and dilated convolutions with different dilation rates to capture the multi-scale structure of rain streaks while maintaining negligible parameter increase. Then, all of the feature maps are concatenated, and Channel Attention (CA) is used to adaptively focus on the important feature information. Last, the convolution is used to output the final result \hat{B} . The decoder structure is the same as the encoder, and the learned content-independent degradation representation is embedded in the decoder feature by MSIBlock.

After obtaining the pre-trained DAEncoder E , we freeze it and retrain the deraining network D , which can be expressed as:

$$\mathcal{L}_D(B, \hat{B}) = \mathcal{L}(B, D(R, deg)) \quad (4)$$

where R and B denote the input of the original rainy image and its corresponding clean image.

Multi-Scale Interaction Block. To make full use of the multi-scale degradation representation learned by DAEncoder to enhance

the structural details and decouple the rain streaks, we propose to embed latent degradation representation into the deraining network. One simple solution is concatenation, but such an operation cannot effectively exploit learned degradation representation to extract complicated rain streaks and may cause optimization interference. Therefore, we propose the MSIBlock for adaptive information interaction. Specifically, we first utilize convolutions to align the content-independent degradation representation deg and content-dependent decoder features \mathcal{F}_r of the deraining network, and then Channel Attention (Att) is used to adaptively enhance the important interactive information, as shown in Fig.1 (a). Last, diverse combinations of Residual Blocks (RB) can further reconstruct the detail of the image. The MSIBlock can be denoted as:

$$\begin{aligned} \mathcal{F}_c &= \text{Att}(\text{Concat}(\text{Conv}(\mathcal{F}_r), \text{Conv}(deg))) \\ \hat{\mathcal{F}} &= \text{Concat}(\text{RB}(\mathcal{F}_c)) \end{aligned} \quad (5)$$

where \mathcal{F}_c and $\hat{\mathcal{F}}$ denotes the concated and the output feature. The MSIBlock is also used in the constraint framework for feature fusion.

3.3. Loss Function

The total training loss $\mathcal{L}_{\text{total}}$ can be formulated as follows:

$$\mathcal{L}_{\text{total}} = \lambda_1 \mathcal{L}_D(B, \hat{B}) + \lambda_2 \mathcal{L}_C(R, \hat{R}) \quad (6)$$

where λ_1 and λ_2 denote the balancing parameters. Following previous work [30, 31, 11], we use MSELoss as \mathcal{L} .

4. EXPERIMENTS

4.1. Implementation Details

In our experiment, we set the training patch size to 256×256 and set λ_1 and λ_2 to 1 and 1. We use the Adam optimizer with an initial learning rate 3×10^{-4} for training our methods on four NVIDIA GeForce RTX 3090 GPUs at Pytorch. And the learning rate of Adam is steadily decreased to 1×10^{-6} using the cosine annealing strategy.

Table 2. Quantitative comparisons on real-world rainy images.

	RESCAN	PReNet	MPRNet	IDT	Ours
NIQE(\downarrow)	3.717	3.543	3.675	3.549	3.487

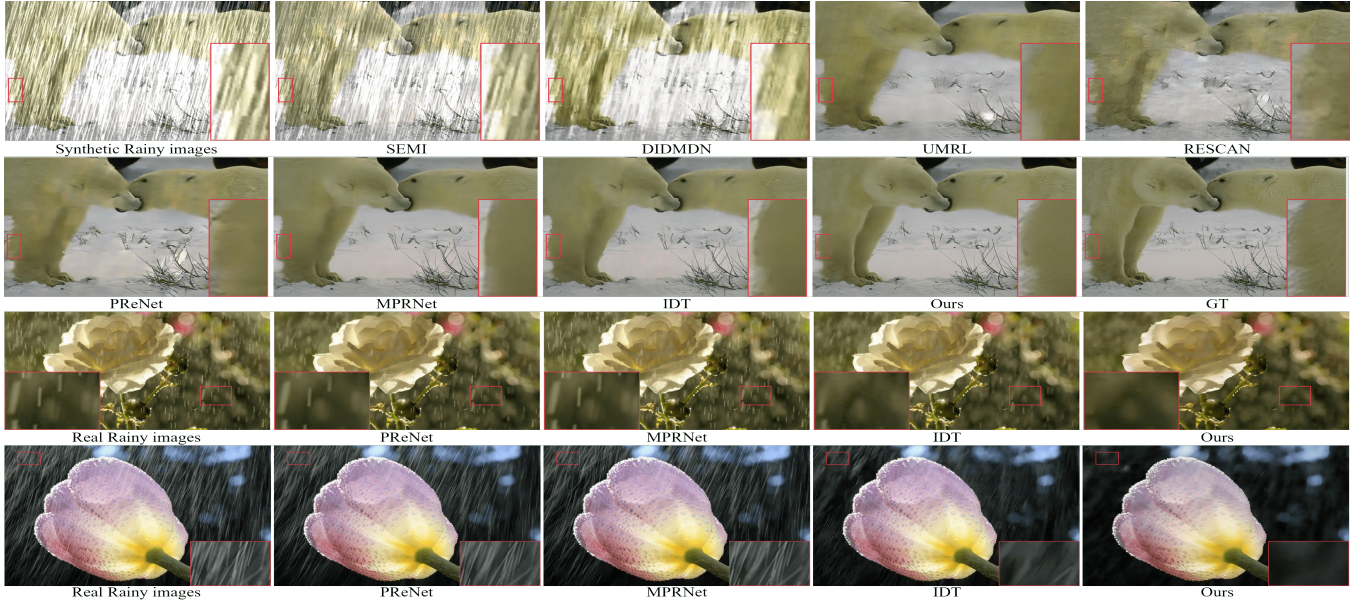


Fig. 2. Visual comparison on the Rain100H [38] and Real15 [38]. The first and second rows compare different methods on a synthetic rainy image. The third and fourth rows are the comparison results on real rainy images. The red boxes are the details of enlarging the local areas.

Table 3. Ablation studies on different settings.

	S1	S2	S3	S4	S5	Ours
PSNR(\uparrow)	27.52	28.37	29.43	29.89	29.96	30.60
SSIM(\uparrow)	0.847	0.865	0.873	0.879	0.878	0.892

4.2. Datasets and Compared Methods

Following [31, 32], we conduct experiments on the Rain13k dataset, which contains 13,712 images with rain streaks of various scales and directions for training, and Test100 [39], Rain100H [38], Rain100L [38], Test1200 [30] and Test2800 [35] are used as test data to evaluate the deraining performance. Real datasets are also considered to test the generalization. We compare our method with existing state-of-the-art deraining methods, including DerainNet [35], SEMI [24], DIDMDN [30], UMRL [25], RESCAN [26], SPANet [10], PReNet [27], MSPFN [31], CRDNet [11], MPRNet [32], IDLIR [14], Uformer-B [13], IDT [34] and Semi-SwinDerain [36]. Continuing along the trajectory of previous works [34, 32, 27], we use PSNR [40] and SSIM [41] to evaluate the deraining performance of synthetic images, and use NIQE [42] to evaluate the real dataset.

4.3. Quantitative and Qualitative Experiment

To quantitatively demonstrate the superiority of our method, we compare our method with several existing SOTA methods, and the results are shown in Tab. 1 and Tab. 2. Our method achieves the best results on the average performance of five test datasets and the best performance on real-world scenarios, which demonstrates that our method achieves good robustness and generalization in real-world scenarios. In addition, we also perform visual comparisons on the Rain100H and Real15 datasets, as shown in Fig. 2. Compared with existing methods, we can observe that our method removes rain streaks more completely and restores better texture details of the background, while other approaches retain some obvious rain streaks or lose important details of the background.

4.4. Ablation study

To verify each proposed component of our model, we perform ablation studies on the Rain100H: S1: Without deraining network, and we use convolutions to map the content-independent degradation representation to rain residual; S2: Without the DAEncoder and the constraint framework; S3: Without constraint framework; S4: Using vanilla convolution to replace the deformable convolution; S5: Using concatenation to replace the MSIBlock. In Tab. 3, we can observe that all components are crucial for our LDRCNet. For example, comparing S1, S2 and our method, which demonstrates content-independent degradation representation and content-dependent features are indispensable for single image deraining. The performance of the proposed method degrades 1.17dB and 0.019 on PSNR and SSIM without the constraint, demonstrating the superiority of our constraint strategy. The performance degrades 0.71dB and 0.013 on PSNR and SSIM without the deformable convolution, demonstrating that direction-aware information is helpful for decoupling rainy patterns effectively. The performance degrades 0.64dB and 0.014 on PSNR and SSIM without the MSIBlock, demonstrating that adaptive information interaction is critical to removing rainy patterns.

5. CONCLUSION

In this paper, we propose a novel LDRCNet for single image deraining, which uses a DAEncoder to learn the latent degradation representation of rain streaks and a constraint framework to provide an explicit guide. To make the well-learned latent degradation representation contribute to the deraining network, we propose the MSI-Block for adaptive information interaction, which helps to remove spatially varying rain patterns adaptively. The proposed network is evaluated on public deraining datasets, including both synthetic and real, demonstrating that the LDRCNet has better performance compared with several representative SOTA methods.

6. REFERENCES

- [1] Chen Zhang, Zefan Huang, Beatrix Xue Lin Tung, Marcelo H Ang, and Daniela Rus, “Smartrainnet: Uncertainty estimation for laser measurement in rain,” in *ICRA*. IEEE, 2023, pp. 10567–10573.
- [2] Jian Chen, Wei Wang, Junxin Chen, and Ming Cai, “Dynamic vehicle graph interaction for trajectory prediction based on video signals,” in *ICASSP*. IEEE, 2023, pp. 1–5.
- [3] Long Peng, Aiwen Jiang, Haoran Wei, Bo Liu, and Mingwen Wang, “Ensemble single image deraining network via progressive structural boosting constraints,” *SPIC*, vol. 99, pp. 116460, 2021.
- [4] Yuntong Ye, Yi Chang, Hanyu Zhou, and Luxin Yan, “Closing the loop: Joint rain generation and removal via disentangled image translation,” in *CVPR*, 2021, pp. 2053–2062.
- [5] Qiaosi Yi, Juncheng Li, Qinyan Dai, Faming Fang, Guixu Zhang, and Tiejong Zeng, “Structure-preserving deraining with residue channel prior guidance,” in *ICCV*, 2021, pp. 4238–4247.
- [6] Yang Wang, Long Peng, Liang Li, Yang Cao, and Zheng-Jun Zha, “Decoupling-and-aggregating for image exposure correction,” in *CVPR*, 2023, pp. 18115–18124.
- [7] Siyuan Li, Iago Breno Araujo, Wenqi Ren, Zhangyang Wang, Eric K Tokuda, Roberto Hirata Junior, Roberto Cesar-Junior, Jiawan Zhang, Xiaojie Guo, and Xiaochun Cao, “Single image deraining: A comprehensive benchmark analysis,” in *CVPR*, 2019, pp. 3838–3847.
- [8] Yu Li, Robby T Tan, Xiaojie Guo, Jiangbo Lu, and Michael S Brown, “Rain streak removal using layer priors,” in *CVPR*, 2016, pp. 2736–2744.
- [9] Lei Zhu, Chi-Wing Fu, Dani Lischinski, and Pheng-Ann Heng, “Joint bi-layer optimization for single-image rain streak removal,” in *ICCV*, 2017, pp. 2526–2534.
- [10] Tianyu Wang, Xin Yang, Ke Xu, Shaozhe Chen, Qiang Zhang, and Rynson W.H. Lau, “Spatial attentive single-image deraining with a high quality real rain dataset,” in *CVPR*, 2019, pp. 12262–12271.
- [11] Long Peng, Aiwen Jiang, Qiaosi Yi, and Mingwen Wang, “Cumulative rain density sensing network for single image derain,” *SPL*, vol. 27, pp. 406–410, 2020.
- [12] Zhifeng Wang, Aiwen Jiang, Chunjie Zhang, Hanxi Li, and Bo Liu, “Self-supervised multi-scale pyramid fusion networks for realistic bokeh effect rendering,” *Journal of Visual Communication and Image Representation*, vol. 87, pp. 103580, 2022.
- [13] Zhendong Wang, Xiaodong Cun, Jianmin Bao, Wengang Zhou, Jianzhuang Liu, and Houqiang Li, “Uformer: A general u-shaped transformer for image restoration,” in *CVPR*, 2022, pp. 17683–17693.
- [14] Mingyu Ma, Dongwei Ren, and Yajun Yang, “Integrating degradation learning into image restoration,” in *ICME*. IEEE, 2022, pp. 1–6.
- [15] Syed Waqas Zamir, Aditya Arora, Salman Khan, Munawar Hayat, Fahad Shahbaz Khan, and Ming-Hsuan Yang, “Restormer: Efficient transformer for high-resolution image restoration,” in *CVPR*, 2022, pp. 5728–5739.
- [16] Yang Wang, Yang Cao, Zheng-Jun Zha, Jing Zhang, and Zhiwei Xiong, “Deep degradation prior for low-quality image classification,” in *Proceedings of the IEEE/CVF Conference on Computer Vision and Pattern Recognition*, 2020, pp. 11049–11058.
- [17] Jifeng Dai, Haozhi Qi, Yuwen Xiong, Yi Li, Guodong Zhang, Han Hu, and Yichen Wei, “Deformable convolutional networks,” in *ICCV*, 2017, pp. 764–773.
- [18] Yang Liu, Ziyu Yue, Jinshan Pan, and Zhixun Su, “Unpaired learning for deep image deraining with rain direction regularizer,” in *ICCV*, October 2021, pp. 4753–4761.
- [19] Ashutosh Kulkarni and Subrahmanyam Murala, “Aerial image dehazing with attentive deformable transformers,” in *WACV*, January 2023, pp. 6305–6314.
- [20] Juntao Guan, Rui Lai, Yang Lu, Yangang Li, Huanan Li, Lichen Feng, Yintang Yang, and Lin Gu, “Memory-efficient deformable convolution based joint denoising and demosaicing for uhd images,” *TCSVT*, vol. 32, no. 11, pp. 7346–7358, 2022.
- [21] Yang Wang, Jing Zhang, Yang Cao, and Zengfu Wang, “A deep cnn method for underwater image enhancement,” in *ICIP*. IEEE, 2017, pp. 1382–1386.
- [22] Wenhan Yang, Robby T Tan, Shiqi Wang, Yuming Fang, and Jiaying Liu, “Single image deraining: From model-based to data-driven and beyond,” *TPAMI*, vol. 43, no. 11, pp. 4059–4077, 2020.
- [23] Yinglong Wang, Shuaicheng Liu, Chen Chen, and Bing Zeng, “A hierarchical approach for rain or snow removing in a single color image,” *TIP*, vol. 26, no. 8, pp. 3936–3950, 2017.
- [24] Wei Wei, Deyu Meng, Qian Zhao, Zongben Xu, and Ying Wu, “Semi-supervised transfer learning for image rain removal,” in *CVPR*, 2019, pp. 3877–3886.
- [25] Rajeev Yasarla and Vishal M Patel, “Uncertainty guided multi-scale residual learning-using a cycle spinning cnn for single image de-raining,” in *CVPR*, 2019, pp. 8405–8414.
- [26] Xia Li, Jianlong Wu, Zhouchen Lin, Hong Liu, and Hongbin Zha, “Recurrent squeeze-and-excitation context aggregation net for single image deraining,” in *ECCV*, 2018, pp. 254–269.
- [27] Dongwei Ren, Wangmeng Zuo, Qinghua Hu, Pengfei Zhu, and Deyu Meng, “Progressive image deraining networks: A better and simpler baseline,” in *CVPR*, 2019, pp. 3937–3946.
- [28] Hong Wang, Zongsheng Yue, Qi Xie, Qian Zhao, Yefeng Zheng, and Deyu Meng, “From rain generation to rain removal,” in *CVPR*, 2021, pp. 14791–14801.
- [29] Xiang Chen, Hao Li, Mingqiang Li, and Jinshan Pan, “Learning a sparse transformer network for effective image deraining,” in *CVPR*, 2023, pp. 5896–5905.
- [30] He Zhang and Vishal M Patel, “Density-aware single image deraining using a multi-stream dense network,” in *CVPR*, 2018, pp. 695–704.
- [31] Kui Jiang, Zhongyuan Wang, Peng Yi, Chen Chen, Baojin Huang, Yimin Luo, Jiayi Ma, and Junjun Jiang, “Multi-scale progressive fusion network for single image deraining,” in *CVPR*, 2020, pp. 8346–8355.
- [32] Syed Waqas Zamir, Aditya Arora, Salman Khan, Munawar Hayat, Fahad Shahbaz Khan, Ming-Hsuan Yang, and Ling Shao, “Multi-stage progressive image restoration,” in *CVPR*, 2021, pp. 14821–14831.

- [33] Zhifeng Wang and Aiwen Jiang, “A dense prediction vit network for single image bokeh rendering,” in *PRCV*. Springer, 2022, pp. 213–222.
- [34] Jie Xiao, Xueyang Fu, Aiping Liu, Feng Wu, and Zheng-Jun Zha, “Image de-raining transformer,” *TPAMI*, 2022.
- [35] Xueyang Fu, Jiabin Huang, Delu Zeng, Yue Huang, Xinghao Ding, and John Paisley, “Removing rain from single images via a deep detail network,” in *CVPR*, 2017, pp. 3855–3863.
- [36] Chun Ren, Danfeng Yan, Yuanqiang Cai, and Yangchun Li, “Semi-swinderain: Semi-supervised image deraining network using swin transformer,” in *ICASSP*. IEEE, 2023, pp. 1–5.
- [37] Yulun Zhang, Yapeng Tian, Yu Kong, Bineng Zhong, and Yun Fu, “Residual dense network for image super-resolution,” in *CVPR*, 2018, pp. 2472–2481.
- [38] Wenhan Yang, Robby T Tan, Jiashi Feng, Jiaying Liu, Zongming Guo, and Shuicheng Yan, “Deep joint rain detection and removal from a single image,” in *CVPR*, 2017, pp. 1357–1366.
- [39] He Zhang, Vishwanath Sindagi, and Vishal M Patel, “Image de-raining using a conditional generative adversarial network,” *TCSVT*, vol. 30, no. 11, pp. 3943–3956, 2019.
- [40] Quan Huynh-Thu and Mohammed Ghanbari, “Scope of validity of psnr in image/video quality assessment,” *Electronics letters*, vol. 44, no. 13, pp. 800–801, 2008.
- [41] Zhou Wang, Alan C Bovik, Hamid R Sheikh, and Eero P Simoncelli, “Image quality assessment: from error visibility to structural similarity,” *TIP*, vol. 13, no. 4, pp. 600–612, 2004.
- [42] Anish Mittal, Rajiv Soundararajan, and Alan C Bovik, “Making a “completely blind” image quality analyzer,” *SPL*, vol. 20, no. 3, pp. 209–212, 2012.